Iranian Heart Journal; 2023; 24 (2)

Original Article

Investigating the Convergence of Phase Analysis Indices by Gated SPECT MPI With Common Filters and Reconstruction Methods

Ahmad Bitarafan-Rajabi[1], PhD; Fardin Adinehvand[3], MD; Fereydoon Rastgou[2*], MD; Hassan Firoozabadi[2], MD; Hadi Malek[2], MD; Nahid Yaghoobi[2], MD; Maziar Sabouri[2], MS

ABSTRACT

Background: The present study aimed to investigate the agreement and convergence of left ventricular dyssynchrony parameters extracted from phase analysis using GSPECT images under different conditions of filtration and reconstruction.

Methods: The study population included 120 consecutive patients with normal or abnormal GSPECT MPI. All patients underwent a 2-day rest and stress sestamibi GSPECT MPI. The GSPECT images were reconstructed and processed using reconstruction methods including filtered back projection (FBP) with Butterworth (cutoff =0.45, order =5) and Metz (cutoff =0.9, order =6) filters and ordered-subset expectation maximization (OSEM) (subset=4,16; iteration =8) with Gaussian filters. Phase analysis (PA) parameters were evaluated globally and regionally (anterior, inferior, septum, lateral, and apex) in patients with normal MPI and those with abnormal MPI.

Results: According to intraclass correlation (ICC) analysis, there was a significant and robust convergence between the OSEM (4,8) and OSEM (16,8) reconstruction algorithms, both of which were with Gaussian filters (P<0.001). Furthermore, there was a significant and robust convergence between FBP and Butterworth (cutoff =0.45, order =5) and between FBP and Metz (cutoff =0.9, order =6) in measuring PA parameters (P<0.001).

Conclusions: The findings indicated that PA parameter values obtained from GSPECT MPI data with the FBP and OSEM image reconstruction methods were strongly correlated. However, the values of normal patients were dependent on the reconstruction technique. Therefore, reconstruction methods should not be used interchangeably. ***(Iranian Heart Journal 2023; 24(2): 45-54)***

KEYWORDS: MPI, Gated SPECT, Phase analysis, Image reconstruction, Filtration

[1] Cardiovascular Intervention Research Center, Rajaie Cardiovascular Medical and Research Center, Iran University of Medical Sciences, Tehran, IR Iran.
[2] Rajaie Cardiovascular Medical and Research Center, Iran University of Medical Sciences, Tehran, IR Iran.
[3] Department of Nuclear Medicine, School of Medicine, Iran University of Medical Sciences, Tehran, IR Iran.

***Corresponding Author:** Fereydoon Rastgou, MD; Rajaie Cardiovascular Medical and Research Center, Iran University of Medical Sciences, Tehran, IR Iran.
Email: f_rastgou@yahoo.com **Tel:** +982122048173

Received: January 19, 2022 **Accepted:** April 12, 2022

Cardiac resynchronization therapy (CRT) is a promising treatment option in a selected group of heart failure patients. [1] Nonetheless, unfortunately about 30% of patients undergoing this treatment do not respond to this costly and invasive treatment. [2-6]

Recent studies have shown that the therapeutic effects of CRT are directly correlated with the existence of left ventricular (LV) mechanical dyssynchrony. [7-10] Echocardiography is the most widely used method to evaluate LV systolic function. Nevertheless, growing evidence indicates that echocardiography does not reliably predict CRT response. [11]

MRI is also a desirable modality for measuring LV dyssynchrony because it has high resolution and excellent tissue characterization, which help select patients for the CRT process. Still, it also has disadvantages, including low availability, high cost, time-consuming imaging process, and impracticality for patients with ICDs and claustrophobia. [12-14] Therefore, there is a need for new alternative imaging modalities.

Recently, phase analysis (PA) of ECG-gated single-photon emission computed tomography (GSPECT) myocardial perfusion imaging (MPI) has been developed as a valuable technique to assess LV mechanical dyssynchrony. [15,16] In addition, GSPECT MPI is already widely used to examine LV dyssynchrony, LVEF, LV volumes, ischemia, viability, and scar tissue. The potential benefits of this technique include wide availability, automation, and reproducibility. [17,18]

Determining the contrast and convergence between the PA findings with various reconstruction methods can help track the impaired heart better. Currently, 2 principal image reconstruction algorithms exist: filtered back projection (FBP) and ordered-subsets expectation maximization (OSEM). [19-21] Besides reconstruction algorithms, filtering methods are also important determinants of the quality of SPECT images. The use of proper filters reduces image defects and noises. [20-22] Finding proper SPECT image reconstruction methods is significant in nuclear medical imaging. In the present study, we investigated the convergence of PA parameters of LV dyssynchrony measured by 2 different reconstruction algorithms (FBP and OSEM) and filtering methods (Metz, Butterworth, and Gaussian) in patients with normal and abnormal GSPECT MPI.

METHODS

Patients

The present study assessed 120 consecutive patients, 70 with normal and 50 with abnormal GSPECT MPI, admitted to Rajaie Cardiovascular Medical and Research Center in Tehran for eligibility. Visual scan interpretation was performed by at least 2 experienced nuclear medicine physicians. Patients with normal MPI by the semi-quantitative analysis were included if they had a sum stress score (SSS) <4, an ejection fraction (EF) >50%, and no myocardial wall motion or wall thickening abnormality. We excluded patients with a known history of cardiac diseases. Patients with abnormal MPI according to the semi-quantitative method were included if they had SSS ≥4 in at least 1 segment, EF ≤50, end-diastolic volume >120 mL, and end-systolic volume >70 mL. We excluded patients with unexplained arrhythmias and those with poor image quality or artifacts (eg, motion artifact and diaphragmatic attenuation), which impede accurate phase analysis (PA).

The protocol of the current study was reviewed and approved by the Ethics Committee of Iran University of Medical Sciences. Written informed consent was obtained from all the participants.

GSPECT MPI

All the patients underwent a 2-day rest and stress sestamibi GSPECT MPI according to the standard protocols. [23] A weight-adjusted standard dose of 99mTc-Sestamibi (8–12mCi) was administered in each phase of the study. The patients were stressed by either exercise or dipyridamole administration, as was suggested by guidelines. [24] Images were obtained 45 to 60 minutes after the stress phase using a dual-detector SPECT/CT camera (Symbia T2, Siemens Medical Systems) with low-energy high-resolution collimators, a 90° detector configuration, and a non-circular body contoured 180° acquisition arc from the right anterior oblique to the left posterior oblique. Each phase of the gated MPI SPECT study was performed in the step-and-shoot mode with a zoom factor of 1.4, a matrix size of 64×64 (pixel size =6.6 mm), 64 projections (25 s per projection), and a 16-frame fixed acceptance window of 30%. The energy window was set to 20% centered over the 140 keV photopeak, accepting gamma rays of 126 to 154 keV. ECG was monitored during the process to ascertain the maintenance of sinus rhythm.

The SPECT images were reconstructed and processed in the rest phase using various methods of reconstruction, including filtered back projection (FBP) with Butterworth (cutoff =0.45, order =5) and Metz (cutoff =0.9, order =6) filters and OSEM (subset =4,16; iteration =8) with Gaussian filters.

Phase Analysis

The methods that affect the convergence of the PA parameters of SPECT images, phase histogram bandwidth (PHB), phase standard deviation (PSD), and entropy were selected and assessed in patients who had undergone a gated myocardial perfusion scan. Finally, the parameters obtained from PA were evaluated globally and regionally (anterior, inferior, septum, lateral, and apex) in patients with normal MPI and those with abnormal MPI using the Cedars-Sinai quantitative gated SPECT (QGS) software.

Statistical Analysis

Quantitative variables were shown as the mean ± the standard deviation (SD). Categorical variables were described as numbers (%). PA indices were compared between the reconstruction methods using the repeated measures ANOVA tests. Intraclass correlation coefficients (ICCs) were used to assess the convergence of the measured PA parameters. The correlation between the reconstruction methods was considered strong if ICC≥0.75, moderate if 0.5≤ICC<0.75, and weak if ICC<0.5. Two-sided *P* values <0.05 were considered statistically significant.

RESULTS

Fifty patients with abnormal MPI and 70 subjects with normal MPI were included. The characteristics of the patients are shown in Table 1.

Normal MPI patients

PA parameters in different cardiac segments of the normal MPI patients are summarized in Table 2. The differences in PSD, PHB, and entropy values with different reconstruction algorithms and filters were significant in all cardiac segments except the apex. However, a high ICC was found for all PA parameters in each cardiac segment, indicating a strong convergence between these reconstruction algorithms and filters (Table 2). The difference due to different reconstruction and filtration conditions for the normal patients can be seen in Figure 1.

Table 1: Characteristics of the study patients

Variable	Abnormal MPI (n=50)	Normal MPI (n=70)
Age, y	59.0±9.8	53.5±9.4
Gender, male (%)	44 (88.0)	52 (74.3)
BMI	27.9±3.8	29.1±4.3
Symptoms, n (%)		
Atypical chest pain	12 (33.3)	19 (41.3)
Chest pain	3 (8.3)	1 (2.2)
Dyspnea on exertion	11 (30.6)	14 (30.4)
Dyspnea on exertion and atypical chest pain	8 (22.2)	12 (26.1)
Dyspnea on exertion and chest pain	2 (5.6)	0 (0.0)
Risk factors, n (%)		
Positive family history	8 (21.6)	13 (31.0)
Hypertension	18 (48.6)	21 (50.0)
Diabetes	9 (24.3)	7 (16.7)
Hyperlipidemia	18 (48.6)	22 (52.4)
Coronary artery disease	8 (21.6)	0 (0.0)

BMI, Body mass index; MPI, Myocardial perfusion imaging

Table 2: Phase analysis parameters from different reconstruction and filtering methods in normal MPI patients.

Parameter	FBP-Butterworth	FBP-Metz	OSEM 4,8-Gaussian	OSEM 16,8-Gaussian	ICC	*P* value
Global						
Mean	136.4 (133.1-139.8)	136.2 (132.8-139.6)	136.0 (132.4-139.6)	136.4 (132.9-139.9)	0.997 (0.996-0.998)	0.333
PSD	10.7 (9.1-12.2)	9.5 (8.0-10.9)	8.0 (6.7-9.3)	10.4 (8.6-12.2)	0.923 (0.884-0.951)	<0.001
PHB	38.1 (33.3-43.0)	34.5 (30.0-39.0)	32.1 (27.6-36.5)	39.3 (32.9-45.6)	0.927 (0.893-0.952)	<0.001
Entropy	39.4 (37.3-41.4)	36.7 (34.5-38.9)	34.8 (32.5-37.1)	38.7 (36.6-40.9)	0.961 (0.921-0.979)	<0.001
Apex						
Mean	134.2 (130.1-138.3)	134.6 (130.6-138.6)	133.9 (129.0-138.8)	138.3 (130.8-145.8)	0.769 (0.677-0.846)	0.351
PSD	4.0 (2.8-5.1)	3.3 (2.5-4.1)	3.2 (2.4-4.0)	4.3 (2.2-6.4)	0.849 (0.781-0.899)	0.194
PHB	17.1 (12.7-21.4)	15.0 (12.3-17.7)	14.6 (11.9-17.3)	17.7 (11.4-24.1)	0.880 (0.827-0.920)	0.221
Entropy	18.0 (15.0-20.9)	16.3 (13.8-18.9)	15.8 (13.1-18.4)	17.0 (14.0-20.0)	0.943 (0.918-0.962)	0.070
Lateral						
Mean	137.0 (133.5-140.5)	136.9 (133.4-140.4)	136.3 (132.6-140.1)	137.2 (133.4-140.9)	0.992 (0.988-0.994)	0.314
PSD	11.4 (8.9-13.9)	9.9 (7.8-12.1)	7.2 (6.0-8.4)	10.1 (8.2-12.0)	0.900 (0.849-0.935)	<0.001
PHB	39.9 (31.8-47.9)	37.3 (29.3-45.3)	27.7 (23.9-31.5)	36.5 (30.0-43.1)	0.876 (0.818-0.918)	<0.001
Entropy	34.3 (32.0-36.6)	32.7 (30.4-35.0)	31.0 (28.5-33.5)	34.7 (32.4-37.0)	0.939 (0.908-0.961)	<0.001
Inferior						
Mean	136.9 (133.5-140.4)	136.8 (133.3-140.2)	136.1 (132.5-139.8)	136.6 (133.1-140.2)	0.995 (0.993-0.997)	0.091
PSD	8.7 (7.0-10.4)	7.7 (6.2-9.1)	6.3 (5.3-7.3)	8.0 (6.7-9.4)	0.940 (0.909-0.961)	<0.001
PHB	32.1 (26.6-37.6)	28.7 (24.2-33.2)	25.2 (21.6-28.8)	30.0 (25.9-34.1)	0.945 (0.917-0.964)	<0.001
Entropy	33.8 (31.4-36.1)	31.9 (29.3-34.4)	28.8 (26.4-31.3)	32.9 (30.4-35.4)	0.938 (0.900-0.961)	<0.001
Septal						
Mean	138.0 (134.3-141.7)	137.4 (133.7-141.1)	137.0 (133.3-140.7)	137.7 (134.0-141.3)	0.996 (0.994-0.997)	0.016
PSD	7.8 (6.8-8.9)	6.6 (5.7-7.6)	5.5 (4.7-6.3)	7.0 (6.1-8.0)	0.929 (0.881-0.957)	<0.001
PHB	29.3 (26.1-32.5)	25.6 (22.8-28.5)	22.8 (20.0-25.6)	27.7 (24.7-30.6)	0.929 (0.885-0.956)	<0.001
Entropy	32.9 (30.5-35.3)	29.8 (27.4-32.2)	26.2 (23.7-28.7)	31.4 (29.2-33.6)	0.925 (0.860-0.957)	<0.001
Anterior						
Mean	135.4 (131.8-138.9)	135.0 (131.5-138.6)	134.0 (128.9-139.1)	137.4 (132.6-142.2)	0.921(0.886-0.948)	0.162
PSD	8.6 (7.3-9.9)	7.7 (6.5-8.8)	6.4 (5.6-7.2)	8.0 (6.9-9.1)	0.938 (0.902-0.961)	<0.001
PHB	31.5 (27.7-35.4)	28.5 (25.0-31.9)	26.5 (23.8-29.2)	30.7 (27.3-34.1)	0.950 (0.924-0.968)	<0.001
Entropy	34.1 (31.8-36.4)	31.4 (29.0-33.8)	30.3 (28.0-32.6)	33.7 (31.4-35.9)	0.960 (0.933-0.976)	<0.001

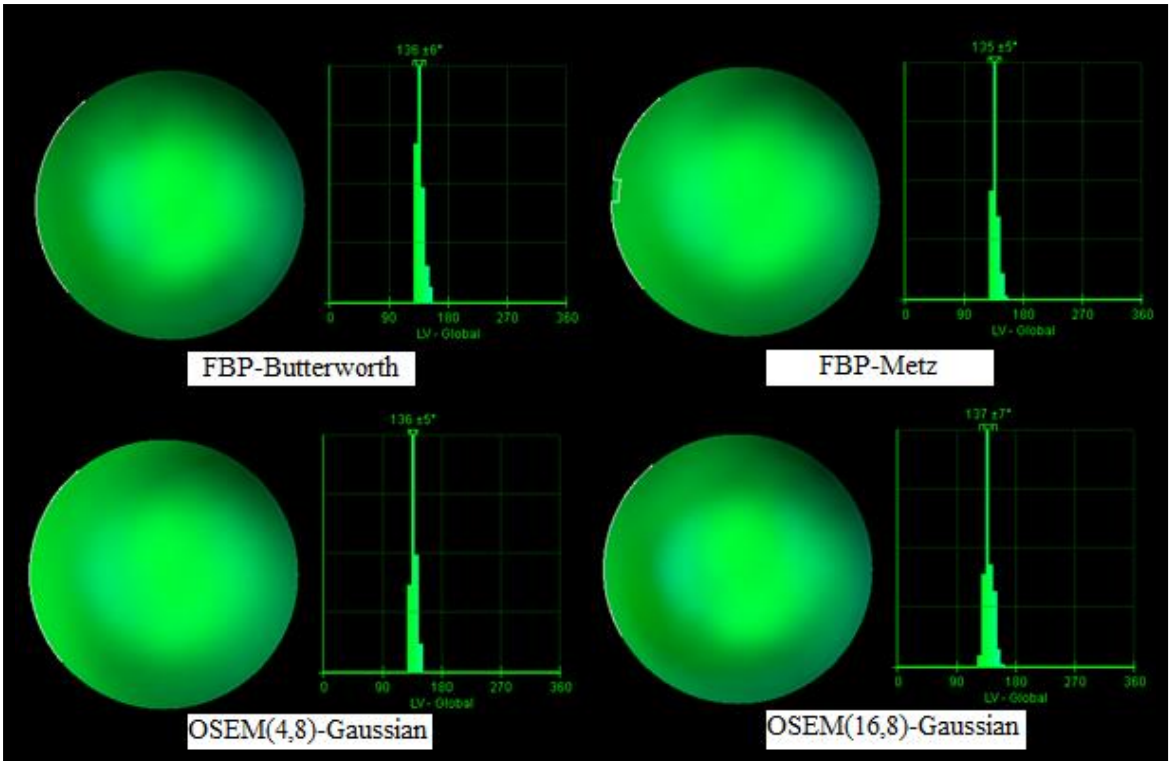

Figure 1: The image depicts phase analysis with different methods of filtering and reconstruction algorithms in global form for scanning normal patients.

Table 3: Phase analysis parameters from different reconstruction and filtering methods in patients with abnormal MPI

Parameter	FBP-Butterworth	FBP-Metz	OSEM 4,8-Gaussian	OSEM 16,8-Gaussian	ICC	*P* value
Global						
Mean	136.5 (132.4-140.5)	136.5 (132.2-140.8)	135.3 (129.0-141.6)	137.1 (132.5-141.8)	0.929 (0.890-0.956)	0.733
PSD	10.8 (9.4-12.2)	9.6 (8.2-10.9)	11.2 (5.9-16.4)	10.2 (8.9-11.4)	0.508 (0.237-0.699)	0.827
PHB	42.8 (37.7-48.0)	39.0 (34.0-44.1)	35.0 (31.0-39.0)	40.7 (36.2-45.2)	0.935 (0.892-0.962)	<0.001
Entropy	40.9 (38.5-43.3)	38.5 (35.8-41.2)	38.1 (35.4-40.8)	41.5 (38.9-44.1)	0.952 (0.918-0.972)	<0.001
Apex						
Mean	134.8 (130.1-139.6)	135.4 (130.4-140.3)	132.8 (125.8-139.7)	134.4 (129.5-139.4)	0.956 (0.932-0.973)	0.346
PSD	4.1 (3.1-5.0)	3.6 (2.7-4.4)	3.4 (2.8-4.0)	4.0 (3.3-4.7)	0.941 (0.908-0.964)	0.008
PHB	17.6 (14.6-20.7)	16.2 (13.3-19.1)	15.8 (13.8-17.9)	17.4 (14.8-20.0)	0.933 (0.897-0.959)	0.109
Entropy	20.6 (17.1-24.1)	18.2 (14.7-21.8)	18.1 (15.1-21.1)	20.8 (18.0-23.6)	0.952 (0.924-0.971)	0.002
Lateral						
Mean	136.2 (131.9-140.5)	142.1 (128.7-155.5)	136.2 (131.8-140.7)	136.5 (132.0-141.0)	0.724 (0.574-0.830)	0.424
PSD	12.7 (6.1-19.3)	8.3 (6.5-10.1)	7.5 (6.1-8.9)	9.5 (7.6-11.5)	0.625 (0.424-0.769)	0.080
PHB	34.9 (28.0-41.8)	30.0 (25.0-35.0)	30.8 (25.7-36.0)	35.5 (29.7-41.4)	0.939 (0.905-0.963)	0.003
Entropy	33.1 (30.6-35.6)	31.1 (28.7-33.6)	32.2 (29.5-34.9)	35.4 (32.6-38.2)	0.919 (0.870-0.951)	<0.001
Inferior						
Mean	136.9 (132.6-141.1)	136.9 (132.3-141.5)	135.6 (130.8-140.4)	136.2 (131.4-141.0)	0.990 (0.984-0.994)	0.159
PSD	8.2 (7.1-9.4)	7.5 (6.4-8.6)	6.9 (5.7-8.1)	8.2 (6.8-9.6)	0.945 (0.914-0.967)	0.001
PHB	32.0 (28.4-35.7)	28.9 (25.2-32.6)	26.8 (22.7-30.8)	31.0 (26.3-35.6)	0.938 (0.901-0.962)	<0.001
Entropy	35.0 (32.0-38.0)	32.0 (28.4-35.6)	30.7 (27.4-34.1)	34.2 (30.9-37.6)	0.939 (0.903-0.963)	<0.001
Septal						
Mean	138.5 (134.0-143.0)	138.4 (133.9-142.8)	136.0 (130.0-141.98)	139.0 (134.4-143.6)	0.937 (0.902-0.961)	0.249
PSD	9.8 (7.7-11.9)	9.3 (6.7-11.9)	7.1 (5.8-8.5)	8.3 (6.9-9.7)	0.877 (0.809-0.925)	0.005
PHB	36.4 (30.0-42.8)	32.4 (26.4-38.4)	31.0 (23.5-38.4)	33.5 (28.2-38.9)	0.826 (0.731-0.893)	0.330
Entropy	35.6 (32.3-39.0)	33.2 (29.2-37.3)	30.3 (26.8-33.8)	35.4 (31.4-39.4)	0.914 (0.864-0.948)	<0.001
Anterior						
Mean	136.3 (132.0-140.5)	133.7 (127.2-140.2)	136.6 (131.9-141.2)	136.7 (132.1-141.2)	0.900 (0.845-0.938)	0.385
PSD	10.1 (8.1-12.0)	9.0 (7.3-10.8)	8.2 (6.9-9.5)	9.9 (7.9-11.8)	0.948 (0.919-0.969	0.001
PHB	40.0 (33.2-46.9)	38.5 (30.2-46.8)	31.1 (27.3-34.9)	35.9 (30.1-41.8)	0.816 (0.716-0.887)	0.024
Entropy	36.7 (33.5-40.0)	35.5 (32.3-38.6)	34.5 (31.7-37.3)	37.2 (34.6-39.8)	0.948 (0.919-0.968)	0.009

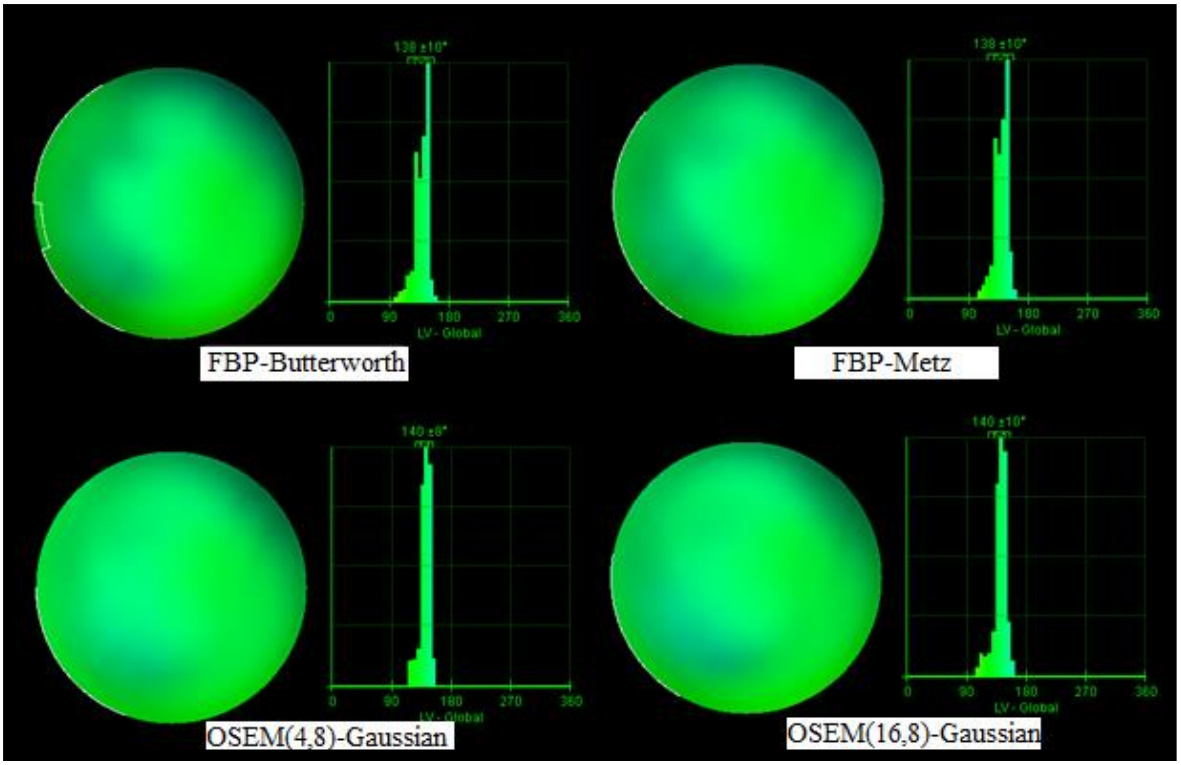

Figure 2: The image illustrates phase analysis with different methods of filtering and reconstruction algorithms in global form for scanning abnormal patients.

Table 4: Phase analysis parameters from different reconstruction and filtering methods in all subjects

Parameter	FBP-Butterworth	FBP-Metz	OSEM 4,8-Gaussian	OSEM 16,8-Gaussian	ICC	*P* value
Global						
Mean	136.4 (133.9-139.0)	136.3 (133.7-139.0)	135.7 (132.4-139.0)	136.7 (133.9-139.5)	0.965 (0.954-0.974)	0.541
PSD	10.7 (9.7-11.8)	9.5 (8.5-10.5)	9.3 (7.0-11.6)	10.3 (9.1-11.4)	0.732 (0.645-0.803)	0.257
PHB	40.1 (36.6-43.6)	36.4 (33.0-39.7)	33.3 (30.2-36.3)	39.9 (35.7-44.0)	0.930 (0.903-0.950)	<0.001
Entropy	40.0 (38.5-41.5)	37.4 (35.8-39.1)	36.2 (34.5-37.9)	39.9 (38.3-41.5)	0.958 (0.928-0.974)	<0.001
Apex						
Mean	134.4 (131.4-137.5)	134.9 (131.8-138.0)	133.4 (129.4-137.4)	136.7 (131.9-141.5)	0.851 (0.802-0.890)	0.298
PSD	4.0 (3.2-4.8)	3.4 (2.8-4.0)	3.3 (2.7-3.8)	4.2 (2.9-5.4)	0.864 (0.819-0.899)	0.030
PHB	17.3 (14.5-20.1)	15.5 (13.5-17.5)	15.1 (13.3-16.9)	17.6 (13.8-21.4)	0.889 (0.853-0.918)	0.053
Entropy	19.0 (16.8-21.3)	17.1 (15.1-19.2)	16.7 (14.8-18.7)	18.6 (16.5-20.7)	0.947 (0.929-0.961)	<0.001
Lateral						
Mean	136.7 (134.0-139.3)	139.0 (133.2-144.9)	136.3 (133.5-139.1)	136.9 (134.1-139.7)	0.840 (0.787-0.882)	0.410
PSD	11.9 (8.9-15.0)	9.3 (7.8-10.7)	7.3 (6.5-8.2)	9.9 (8.5-11.2)	0.761 (0.682-0.824)	<0.001
PHB	37.8 (32.4-43.3)	34.3 (29.2-39.3)	29.0 (25.9-32.1)	36.1 (31.6-40.6)	0.893 (0.857-0.922)	<0.001
Entropy	33.8 (32.1-35.5)	32.1 (30.4-33.7)	31.5 (29.7-33.3)	35.0 (33.2-36.7)	0.931 (0.904-0.951)	<0.001
Inferior						
Mean	136.9 (134.3-139.6)	136.8 (134.1-139.6)	135.9 (133.1-138.8)	136.5 (133.6-139.3)	0.993 (0.990-0.995)	0.012
PSD	8.5 (7.4-9.6)	7.6 (6.6-8.6)	6.6 (5.8-7.3)	8.1 (7.1-9.1)	0.941 (0.917-0.958)	<0.001
PHB	32.1 (28.5-35.6)	28.8 (25.8-31.8)	25.9 (23.2-28.5)	30.4 (27.4-33.5)	0.942 (0.919-0.959)	<0.001
Entropy	34.3 (32.4-36.1)	31.9 (29.8-34.0)	29.6 (27.7-31.6)	33.4 (31.5-35.4)	0.938 (0.910-0.957)	<0.001
Septal						
Mean	138.2 (135.4-141.1)	137.8 (135.0-140.6)	136.6 (133.3-139.8)	138.2 (135.4-141.0)	0.970 (0.960-0.978)	0.054
PSD	8.7 (7.6-9.7)	7.8 (6.5-9.0)	6.2 (5.5-6.9)	7.6 (6.8-8.4)	0.898 (0.860-0.927)	<0.001
PHB	32.3 (29.0-35.5)	28.4 (25.4-31.5)	26.2 (22.7-29.7)	30.1(27.3-32.9)	0.869 (0.826-0.904)	<0.001
Entropy	34.0 (32.0-36.0)	31.2 (29.1-33.4)	27.9 (25.8-30.0)	33.1 (31.0-35.2)	0.921 (0.879-0.947)	<0.001
Anterior						
Mean	135.7 (133.1-138.4)	134.5 (131.1-137.8)	135.1 (131.6-138.6)	137.1 (133.7-140.4)	0.912 (0.883-0.935)	0.165
PSD	9.2 (8.1-10.3)	8.2 (7.2-9.2)	7.2 (6.4-7.9)	8.8 (7.7-9.8)	0.945 (0.921-0.961)	<0.001
PHB	35.1 (31.4-38.7)	32.7 (28.6-36.7)	28.4 (26.2-30.7)	32.9 (29.8-36.0)	0.878 (0.837-0.911)	<0.001
Entropy	35.2 (33.3-37.1)	33.1 (31.2-35.0)	32.1 (30.2-33.9)	35.1 (33.4-36.8)	0.956 (0.937-0.969)	<0.001

Abnormal MPI patients

There was no significant difference between PSD calculated via different reconstruction algorithms and filters globally and in the lateral cardiac segment (Table 3). The PHB parameter was significantly different in all cardiac segments except in the apex and the septal segments (Table 3). The differences in entropy values with different reconstruction algorithms and filters were significant in all cardiac segments (Table 3). The convergence between the reconstruction algorithms and filters was strong for PHB and entropy indices and moderate to strong for PSD (Table 3). The difference due to different reconstruction and filtration conditions for abnormal patients can be seen in Figure 2.

All subjects

When considering all subjects, PSD, PHB, and entropy parameters varied significantly between different reconstruction algorithms and filters in all cardiac segments except the apex (Table 4). Globally, PSD values were similar between the reconstruction methods (*P*=0.257). In the apex, no significant difference in PHB values was found between different reconstruction algorithms and filters (*P*s=0.053). A strong convergence was found between the reconstruction methods in all cardiac segments (Table 4).

DISCUSSION

Our results show that although there was some difference in PA parameter values derived from GSPECT MPI with various image reconstruction methods, the convergence of these values was found to be moderate to strong across all cardiac segments. To the best of our knowledge, no prior study has evaluated the convergence between PA parameters with different image reconstruction algorithms and filters, so the present study is unique in this regard.

In a study conducted by Li et al, [25] various iterative reconstruction methods were compared with the FBP in measuring LV dyssynchrony in both stress and rest phases. The authors found that the mean PSD and PHB values were quite similar in all of the reconstruction methods. In our study, the main PA parameters' (PSD, PHB, and entropy) values were not significantly different between various reconstruction methods in the normal SPECT MPI population. Be that as it may, in patients with abnormal SPECT MPI and the total study population, PHB and entropy values measured by different reconstruction methods were not similar.

According to previous studies, it seems that the quality of SPECT images is higher with the use of iterative reconstruction methods than FBP. [26] The results from a study conducted by Hatton et al [27] demonstrated that compared with FBP (Butterworth), using OSEM (4, 2) reconstruction method was associated with fewer artifacts and improved tolerance to missing projections. In another study, reconstruction methods OSEM (8, 2) and FBP (Metz) were compared, and the results showed that motion artifacts were greater with the use of the OSEM method. [28] The findings from a study comparing the quality of images reconstructed with the Butterworth, maximum likelihood expectation maximization (MLEM), and OSEM methods indicated the superiority of OSEM. [29]

Won et al [30] compared the interpretations and functional results of GSPECT MPI when images were reconstructed with FBP (Butterworth) and OSEM (2, 12) methods. The results revealed that there was no significant difference in the interpretation of GSPECT MPI, and the functional parameters calculated with FBP and OSEM were strongly correlated. However, there was a statistically significant difference between these methods in functional results. Manish et al [31] compared Butterworth and Metz in the evaluation of end-diastolic volume, end-systolic volume, and EF and found the results were similar and

strongly correlated. In another study by Bitarafan et al, [32] the effect of reconstruction parameters on EF values was investigated by comparing the results with EF calculated by angiography and echocardiography. The FBP reconstruction algorithm overestimated the EF, whereas the use of OSEM was associated with a lower estimation of EF. The EF values calculated with the Metz filtering method and OSEM (12-2) were the most comparable results with echocardiography and angiography. Similarly, Duarte et al [33] showed that applying the FBP and OSEM methods was associated with overestimation and lower estimation of EF, respectively. Still, the authors indicated that the OSEM reconstruction method was superior to FBP in calculating EF.

Limitations

The current study has a salient limitation. We only compared PA parameters derived from GSPECT MPI with different reconstruction methods in a small sample of patients from a single referral center. Therefore, these results should be interpreted cautiously.

CONCLUSIONS

Although the values of PA parameters obtained from GSPECT MPI data varied significantly among different image reconstruction methods, these results were strongly correlated in almost all cardiac segments in both normal and abnormal MPI populations. Nonetheless, the values of normal patients were dependent on the reconstruction technique. Therefore, reconstruction methods should not be used interchangeably. Further studies with larger sample sizes are needed to determine the clinical significance of each reconstruction and filtration method and its association with the prognosis of the patients.

Acknowledgments

Special thanks are due to all our colleagues at Rajaie Cardiovascular Medical and Research Center for their role in this research.

Data Availability Statement

The data that support the findings of this study are available upon reasonable request from the corresponding author.

Disclosure

There is no financial disclosure.

REFERENCES

1. Abraham, W.T. and D.L. Hayes, Cardiac resynchronization therapy for heart failure. Circulation, 2003. 108(21): p. 2596-2603.

2. C. Leclercq and D. A. Kass, “Retiming the failing heart: Principles and current clinical status of cardiac resynchronization,” J. Am. Coll. Cardiol., vol. 39, no. 2, pp. 194–201, 2002, doi: 10.1016/S0735-1097(01)01747-8.

3. W. T. Abraham and D. L. Hayes, “Cardiac Resynchronization Therapy for Heart Failure,” Circulation, vol. 108, no. 21, pp. 2596–2603, 2003, doi: 10.1161/01.CIR.0000096580.26969.9A.

4. C. Leclercq and J. M. Hare, “Ventricular Resynchronization: Current State of the Art,” Circulation, vol. 109, no. 3, pp. 296–299, 2004, doi: 10.1161/01.CIR.0000113458.76455.03.

5. A. Auricchio et al., “Effect of pacing chamber and atrioventricular delay on acute systolic function of paced patients with congestive heart failure,” Circulation, vol. 99, no. 23, pp. 2993–3001, 1999, doi: 10.1161/01.CIR.99.23.2993.

6. E. C. Adelstein and S. Saba, “Scar burden by myocardial perfusion imaging predicts echocardiographic response to cardiac resynchronization therapy in ischemic cardiomyopathy,” Am. Heart J., vol. 153, no. 1, pp. 105–112, 2007, doi:

7. Bax, J.J., et al., Left ventricular dyssynchrony predicts response and prognosis after cardiac resynchronization therapy. Journal of the American College of Cardiology, 2004. 44(9): p. 1834-1840.

8. Yu, C.M., et al., Tissue Doppler echocardiographic evidence of reverse remodeling and improved synchronicity by simultaneously delaying regional contraction after biventricular pacing therapy in heart failure. Circulation, 2002. 105(4): p. 438-45.

9. Bax, J.J., et al., Left ventricular dyssynchrony predicts benefit of cardiac resynchronization therapy in patients with end-stage heart failure before pacemaker implantation. The American Journal of Cardiology, 2003. 92(10): p. 1238-1240.

10. Shojaeifard M, Ghaedian T, Yaghoobi N, Malek H, Firoozabadi H, Bitarafan-Rajabi A, et al. Comparison of Gated SPECT Myocardial Perfusion Imaging with Echocardiography for the Measurement of Left Ventricular Volumes and Ejection Fraction in Patients With Severe Heart Failure. Research in cardiovascular medicine. 2016;5(1):e29005.

11. Chung, E.S., et al., Results of the Predictors of Response to CRT (PROSPECT) trial. Circulation, 2008. 117(20): p. 2608-16.

12. M. M. Henneman et al., "Can LV dyssynchrony as assessed with phase analysis on gated myocardial perfusion SPECT predict response to CRT?," J. Nucl. Med., vol. 48, no. 7, pp. 1104–1111, 2007, doi: 10.2967/jnumed.107.039925.

13. H. Abu Daya, S. Malhotra, and P. Soman, "Radionuclide Assessment of Left Ventricular Dyssynchrony," Cardiol. Clin., vol. 34, no. 1, pp. 101–118, 2016, doi: 10.1016/j.ccl.2015.08.006.

14. C. Stellbrink, O. Breithardt, A. Sinha, P. Hanrath, M. K. I, and K. D. R. Aachen, "How to discriminate responders from non-responders to cardiac resynchronisation therapy," vol. 6, pp. 101–105, 2004, doi: 10.1016/j.ehjsup.2004.05.008.

15. Chen, J., et al., Onset of left ventricular mechanical contraction as determined by phase analysis of ECG-gated myocardial perfusion SPECT imaging: Development of a diagnostic tool for assessment of cardiac mechanical dyssynchrony. Journal of Nuclear Cardiology, 2005. 12(6): p. 687-695.

16. Rastgou F, Shojaeifard M, Amin A, Ghaedian T, Firoozabadi H, Malek H, et al. Assessment of left ventricular mechanical dyssynchrony by phase analysis of gated-SPECT myocardial perfusion imaging and tissue Doppler imaging: comparison between QGS and ECTb software packages. Journal of nuclear cardiology : official publication of the American Society of Nuclear Cardiology. 2014;21(6):1062-71.

17. N. Tao et al., "Assessment of left ventricular contraction patterns using gated SPECT MPI to predict cardiac resynchronization therapy response," J. Nucl. Cardiol., vol. 25, no. 6, pp. 2029–2038, 2018, doi: 10.1007/s12350-017-0949-1.

18. M. M. Boogers, J. Chen, and J. J. Bax, "Role of nuclear imaging in cardiac resynchronization therapy," Expert Rev. Cardiovasc. Ther., vol. 7, 2009, doi: 10.1038/nrcardio.2009.189.

19. Bruyant, P.P., Analytic and Iterative Reconstruction Algorithms in SPECT. Journal of Nuclear Medicine, 2002. 43(10): p. 1343-1358.

20. Bitarafan Rajabi, H Rajabi, N Yaghoobi, F Rastgoo, SH Firoozabadi. Filter selection for 99mTc-Sestamibi myocardial perfusion SPECT imaging [Persian]. A Iranian Journal of Nuclear Medicine 11 (1), 41-50

21. H Rajabi, AB Rajabi, N Yaghoobi, H Firouzabad, F Rustgou. Determination of the optimum filter function for Tc99m-sastamibi myocardial perfusion SPECT imaging. Indian Journal of Nuclear Medicine 20 (3), 77-82

22. Lyra, M. and A. Ploussi, Filtering in SPECT image reconstruction. Journal of Biomedical Imaging, 2011. 2011: p. 10.

23. Zaret, B.L. and G.A. Beller, Clinical Nuclear Cardiology: State of the Art and Future Directions E-Book. 2010: Elsevier Health Sciences.

24. Henzlova MJ, Duvall WL, Einstein AJ, Travin MI, Verberne HJ. ASNC imaging guidelines for SPECT nuclear cardiology procedures: Stress, protocols, and tracers. Journal of nuclear cardiology: official

publication of the American Society of Nuclear Cardiology. 2016;23(3):606-39

25. Li, D., et al., Impact of image reconstruction on phase analysis of ECG-gated myocardial perfusion SPECT studies. Nuclear medicine communications, 2009. 30(9): p. 700-705.

26. Lyra, M., et al., Filters in 2D and 3D cardiac SPECT image processing. Cardiology research and practice, 2014. 2014.

27. Hatton, R.L., et al., Improved tolerance to missing data in myocardial perfusion SPET using OSEM reconstruction. European Journal of Nuclear Medicine and Molecular Imaging, 2004. 31(6): p. 857-861.

28. Zakavi, S.R., et al., Image Reconstruction Using Filtered Backprojection and Iterative Method: Effect on Motion Artifacts in Myocardial Perfusion SPECT. Journal of Nuclear Medicine Technology, 2006. 34(4): p. 220-223.

29. Modi, B.N., et al., A qualitative and quantitative assessment of the impact of three processing algorithms with halving of study count statistics in myocardial perfusion imaging: filtered backprojection, maximal likelihood expectation maximisation and ordered subset expectation maximisation with resolution recovery. J Nucl Cardiol, 2012. 19(5): p. 945-57.

30. Won, K., et al., Is iterative reconstruction an improvement over filtered back projection in processing gated myocardial perfusion SPECT? The Open Medical Imaging Journal, 2008. 2(1).

31. Manish, O., et al., Do reconstruction filters really effect the volume and ejection fraction calculation with 99Tc-sestamibigated myocardial SPECT? Indian journal of nuclear medicine : IJNM : the official journal of the Society of Nuclear Medicine, India, 2010. 25(4): p. 156-159.

32. Bitarafan, A. and H. Rajabi, The effect of filtrating and reconstruction method on the left ventricular ejection fraction derived from GSPET: a statistical comparison of angiography and echocardiography. Ann Nucl Med, 2008. 22(8): p. 707-13.

33. Duarte, D.D., et al., Influence of reconstruction parameters during filtered backprojection and ordered-subset expectation maximization in the measurement of the left-ventricular volumes and function during gated SPECT. J Nucl Med Technol, 2012. 40(1): p. 29-36.